Quantification of Hyperhidrosis using Electronic Sudometer

SYED GHUFRAN KHALID

KTH Industrial Engineering
and Management

Master of Science Thesis in Medical Engineering
Stockholm, Sweden 2013

Quantification of Hyperhidrosis using Electronic Sudometer

SYED GHUFRAN KHALID

Master of Science Thesis, 30 credits

Supervisor: Assoc. Prof. Stig Ollmar,
Karolinska Institutet, CLINTEC

Examiner: Prof. Birgitta Janerot Sjöberg,
Karolinska Institutet, CLINTEC

TRITA-STH-2013: 105

Royal Institute of Technology
KTH STH
SE-14186 Flemingsberg, Sweden

ABSTRACT

Human skin has various pathologies in the form of acute and chronic diseases. Some are only cosmetic diseases which are not harmful for life but they can affect mental health and disrupt daily activities. Hyperhidrosis is one of these cosmetic diseases which may be caused by diabetes, infections, or thyroid hyper activity, or can be inherited. There are some examinations for testing hyperhidrosis, e.g. gravimetric and minor starch-iodine test. There are some devices that can measure sweat but are not specifically used or even intended for use on hyperhidrosis.

A non-invasive prototype instrument called Electronic Sudometer using the principle of electrical impedance measurement has been developed. The philosophy behind this prototype is to make an instrument which can detect hyperhidrosis during homeostasis as well as in pathological condition. The device injects a sinusoid electric current and detects the ensuing voltage, which is proportional to the impedance of sweat on top of the skin during hyperhidrosis. For this prototype, the electrode system is made of brass rings mounted on a handle. The signal is then processed in electronic assembly. Processed output is transferred to a Laptop with specially made connecting wire. Computer having Sound Card Oscilloscope (Lab View based software) plots the signal and shows voltage level corresponding to sudor level. The signal output can also be displayed on a SmartPhone having software called Osciprime, requiring another specially made interface.

Laboratory test results in the form of a plot of output voltage vs. impedance show accuracy of the device. The impedance results can be translated to sweat level because impedance decreases with increasing sweat during hyperhidrosis. The Sudometer was also calibrated using fixed precision resistors over its working range. Laboratory tests were carried out using an artificial skin at various sweat levels and to a yeast tissue model. Hydration of the artificial skin was quantified by weighing precision cut samples on a laboratory balance. Results from two test persons (the author and a student friend) are also included in this Master Thesis. During these experiments, the laptop computer and SmartPhone, respectively, were on internal battery to eliminate electric hazard.

Any clinical device must be validated for accuracy and evaluated for safety before applying it on patients – the latter has not been done with the prototype. The author is aware of potential electrical risks, and thus the whole system was disconnected from mains 230V during measurements on himself and a student friend. The device output seems to be well correlated to sweat level although electrolytes were not taken into account. Being a palmar hyperhidrosis patient himself, the author applied the Electronic Sudometer on his palms and the results look quite promising. At different environmental temperatures, the author checked elicited sweat responses. Patient safety is always a concern for clinicians regarding new devices. For this reason, the device itself has been made battery operated, and a new version will be entirely powered from a SmartPhone.

Acknowledgement

First of all I like to thank All Mighty Allah for giving me the strength to complete this Master Thesis.

I want to express my sincere gratitude to my supervisor Associate Professor Stig Ollmar, Karolinska Institutet, for believing in me and guiding me on each and every step of this Master's thesis. Without his support, fruitful discussion, positive criticism and encouragement I couldn't think to make the Electronic Sudometer. I really appreciate his suggestion to pursue advancement of the device after this Master's thesis to become a medical product.

I am really thankful to the KTH – Royal Institute of Technology, School of Technology and Health, department of Medical Engineering to allow this Master's thesis. I am grateful to CLINTEC, Karolinska Institutet, Division of Medical Imaging and Engineering, for providing me facilities to work on my Master's Thesis, in particular granting me access to their electronics lab, which was an essential requirement to create the Electronic Sudometer. I like to thank Dr. Anna Bjällmark for giving me access to a precision lab scale and pipett, which were very important for accurate measurement of samples. I am really thankful to Satya Vasu for training of pippetting and using the electronic scale during sampling. I like to thank Peter Arfert who helped with mechanical assembly of the probe. Special thanks to Dr. Carl Swartling and Dr. Alma Rystedt at Svettmottagningen, S:t Göran Hospital for inspiring discussions. Thank you SciBase AB for giving me access to the reference Agilent impedance meter while mapping typical ranges of expected values during initial impedance readings, before designing the circuits of the Sudometer. I also like to thank my friends Muhammad Asim Faridi, Adnan Faqui Shahzad and Sharifuzaman Khan, who provided me support as well as encouragement during the design of this device.

A big thank to my parents, specially my mother for giving me the opportunity and financial support for my higher education. Without them I couldn't have reached KTH for Master's Studies. Thank you Shahina Aunty for supporting me during my higher education. I like to thank my younger brothers S. Abdul Rahim, S. Sheraz Khalid and S. Khizr for giving me confidence during this Master's Thesis.

Finally, I like to thank my lovely wife Madiha. She just joined me in marriage, and she supports and encourages me to continue my work towards PhD by pursuing this line of research.

Abbreviations

ADC	Analogue to Digital Converter
CD	Compact Disk
DAC	Digital to Analogue Converter
EBI	Electrical Bioimpedance
ECM	Electrical Capacitance Moist measurement
EPI	Evaporimeter
HH	Hyperhidrosis
MDD	Medical Device Directive
Op Amp	Operational Amplifier
SC	Stratum Corneum
SUT	System Under Test
TEWL	Trans Epidemal Water Loss
TRS	Tip Ring Sleeve
WTX	Wettex

Physical Symbols

A		Amplitude or Area or Gain of amplifier (context dependent)
C		Capacitor
f		Frequency
h		Height
L		Length
m		meter
Q		Quality Factor
R		Resistance
ρ	(Gr. rho)	Resistivity
V		Voltage

Table of Contents

CHAPTER 1

1 INTRODUCTION

Human skin is the largest organ of the body and has various pathologies in the form of acute and chronic diseases. Some are only cosmetic diseases which are not very harmful but they can affect mental health and disrupt daily activities. Some diseases can lead to hyperhydrosis (HH), such as diabetes, some infections, or thyroid hyper activity [1]. There are some tests for HH, e.g. *gravimetric* and *minor starch-iodine* tests. Some devices also measure sweat but they are not much used for HH due to limitations that will be discussed later in this chapter.

This Master Thesis proposes a prototype device which can measure sweat level using electrical bioimpedence (EBI) technique on human skin. A specially designed sensor has been designed for providing patient comfort. Laboratory tests of this instrument have been carried out at KTH using artificial skin materials and models. Promising results lead to testing on a living cell structure, i.e. bakery yeast. Being a HH patient, the author applied the device on himself as well as on a student friend. The instrument was calibrated using with fixed resistors.

1.1 Background

1.1.1 Details about the area of interest

Sweat is a mixture of water 99%, salt 0.2-0.5%, urea traces 0.08%, ammonia, Vitamin C and lactic acid, and has acidic pH in the range 2-6. Sweat could alternatively be called a hypertonic filtrate [2]. Sweating is governed by the sympathetic division of the autonomic nervous system. Strenuous exercise, extreme physical activities, elevated temperature, and mental stress can activate sweating. Sweat glands are responsible for sweat excreted out via excretory pores on the skin.

Sweat pores are found on most areas of the human skin. On the back, the density is approximately 60-80 pores/cm^2, and palms have around 400 pores/cm^2. Sweat glands are of two types, *eccrine* which are large in numbers especially on palms, soles and forehead. Another type is called *apocrine* and are mostly found in axillary and genital areas. In this thesis, only *eccrine* sweating has been studied.

1.1.2 Hyperhidrosis

HH denotes excessive secretion of the sweat glands [3]. A patient may sweat even in a cool environment or in resting condition [4]. It is not a rare problem, but most people don't know about this problem [5]. We can classify HH in two types.

1. Primary or focal HH
2. Secondary HH

Primary HH affects the hands, feet or axillae. Secondary HH is also called generalized HH which is caused by hyperthyroidism, infections, diabetes Mellitus, food having high spices, and coffee or chocolate.

Figure 1: Palmar Hyperhidrosis

This Master thesis project is focused on Primary HH which is depicted in Figure 1. Statisticians report 1% of the population has such kind of disease [6]. In the US 2.8% of the population has focal HH but of these only 38% consult health professionals [7]. Usually patients feel social embarrassment and considerable burden in their activities from extreme sweating [5,6-9]. It is believed that it is related to the over-stimulation of autonomic pathways. We can differentiate the palmar HH into mild, moderate and severe. In mild palmar HH, sweat droplets are not visible on the wet palm. In moderate situation, sweating area broadens to fingertips. In severe cases, droplets of sweat become visible [10,11].

1.1.3 Previous Quantification Techniques

Sweat quantification tests or the mapping of sweating area are used in clinical examinations for the assessment of treatment responses. The most common tests for sweat monitoring are *Gravimetric Analysis* and the *Minor starch-iodine* tests [11].

1.1.3.1 Gravimetric Test

It requires a filter paper which after weighting in dry condition is placed for 60 seconds on the skin, enough to absorb the sweat on the skin. Thereafter the weight of the paper is again measured. Sweat rate can be calculated as mg/min/cm^2 [11]. In Table 1, HH results are compared with normal sweat rates.

Table 1: Sweat Rate [12]

Anatomic Area	**"Normal" based on clinical trials**	**Criteria for Diagnosis of Hyperhidrosis**
Axilla: Males	Average 14.4 mg/min/cm^2	> 20 mg/min/cm^2
Axilla: Females	Average 9.4 mg/min/cm^2	> 10 mg/min/cm^2
Palm	< 20 mg/min/cm^2	> 30-40 mg/min/cm^2

Minor Starch-Iodine test

In this test 1-5% iodine solution is applied to the target area and left to dry. After a few seconds, starch is powdered over the dried iodine solution [13]. Sweat changes colour from brown to purple because of the complex formed by the iodine and starch, which can be seen in Figure 3. Then serial photographs can be taken for documentation.

There are other bioengineering techniques which are not specific for HH but can measure sweat, including Transepidermal Water Loss (TEWL) and Electrical Capacitance Moist measurement (ECM). [14]. There is also an instrument named SudoLogger (BioGauge AG, Oslo, Norway) which measures filling of sweat ducts using principles of EBI.

1.1.3.2 Transepidermal Water Loss (TEWL)

Passive diffusion of water through the skin leaves from the surface of the *stratum corneum* (SC). It can be measured by e.g. the original Swedish invention Evaporimeter EPI (Servomed AB, Kinna, Sweden), or similar devices. It is primarily used to quantify skin barrier status. The EPI measures water vapor evaporated from the skin through a perpendicular open chamber, like through a chimney. After the level has been stabilized, readings can be taken after 30-60s [15,16]. Some TEWL devices use closed chamber, e.g. the VapoMeter (Delfin Technologies, Kuopio, Finland). According to International guidelines (2013), closed chamber instruments are now preferred since they are less vulnerable to artifacts [17].

1.1.3.3 Electrical Capacitance Moist Measurement

Corneometer CM820 (Courage and Khazaka GmbH, Cologne, Germany) uses a principle of electrical capacitance moist detection. This device detects capacitance at relatively low frequency. The probe of Corneometer covers 49mm^2, and is applied to the skin with 3.5N force. Recording time is 3 seconds and results are given in arbitrary units. It indirectly measures hydration of the SC by measuring capacitance created by the interdigitated electrodes on the probe surface and the

dielectric medium in the vicinity of these [14,16,18,19]. The Corneometer is well suited for small changes in normal skin hydration, e.g. for testing of efficacy of various skin moisturizers.

1.1.3.4 Other techniques

Already 1890, Tarchanoff discovered the Psycho-Galvanic Reflex (sometimes called Galvanic Skin Response, GSR), and suggested that changes in skin electrical resistance was caused by changes in secretory activity of the sweat glands. [20]. This correlation has been exploited in various types of so called "lie detectors", and Keeler seems to have been the first to include GSR with other physiological parameters like blood pressure, pulse rate and breathing for this purpose [21]. SudoLogger (BioGauge AG, Oslo, Norway) is a new instrument based on EBI and detects filling of sweat ducts, and is intended for use in medicine, sports, psychology, and physiological research. The principle is described in [22].

1.1.3.5 Present Innovation

Efforts made at both the Karolinska Institute and at KTH resulted in a prototype device which can detect sweat caused by HH. The intended use is quantification of rich amounts of sweat, much more than filling of sweat ducts. This prototype can easily be further developed into a product complying with the Medical Device Directive (MDD), and with professional design due to its small sized hardware and interfaces for Laptops and SmartPhones.

CHAPTER 2

2 GOALS

The design of this prototype HH-meter has to meet some clinical requirements. A sensor that interfaces with skin and sweat should not itself be a cause of heating or irritation around the sensor, as that would introduce errors in the measurements. Thus:

- Designing a prototype sensor having accuracy to detect high amount of sweat present on skin.
- Designing of electronic hardware for prototype
- Designed prototype should interface with Laptop

Optional Goal

- Designed prototype can be interfaced to a SmartPhone.

CHAPTER 3

3 METHODOLOGY

A non invasive prototype instrument using the principle of electrical impedance measurement at one frequency is developed. The notion behind this prototype is to make an instrument which can detect HH during homeostasis. This complete prototype instrument consists of a dry metal electrode probe connected with an electronic module. The sensor injects a current in the form of a sinusoid into the sweat layer on top of the skin and the ensuing voltage between the sensor electrodes will be inversely proportional to the sweat amount. This signal is then processed in the analog electronic assembly. Processed analog output is then sent to the Laptop sound card via a dedicated connecting wire. At this point further signal processing is performed digitally in the sound card and displayed using a software called *Sound Scope*. This signal output can also be displayed on a Smart Phone, which interface requires another dedicated connecting wire. The signal will then be displayed on the Smart phone using software called *Osciprime*. Signal flow diagram is shown in Figure 2.

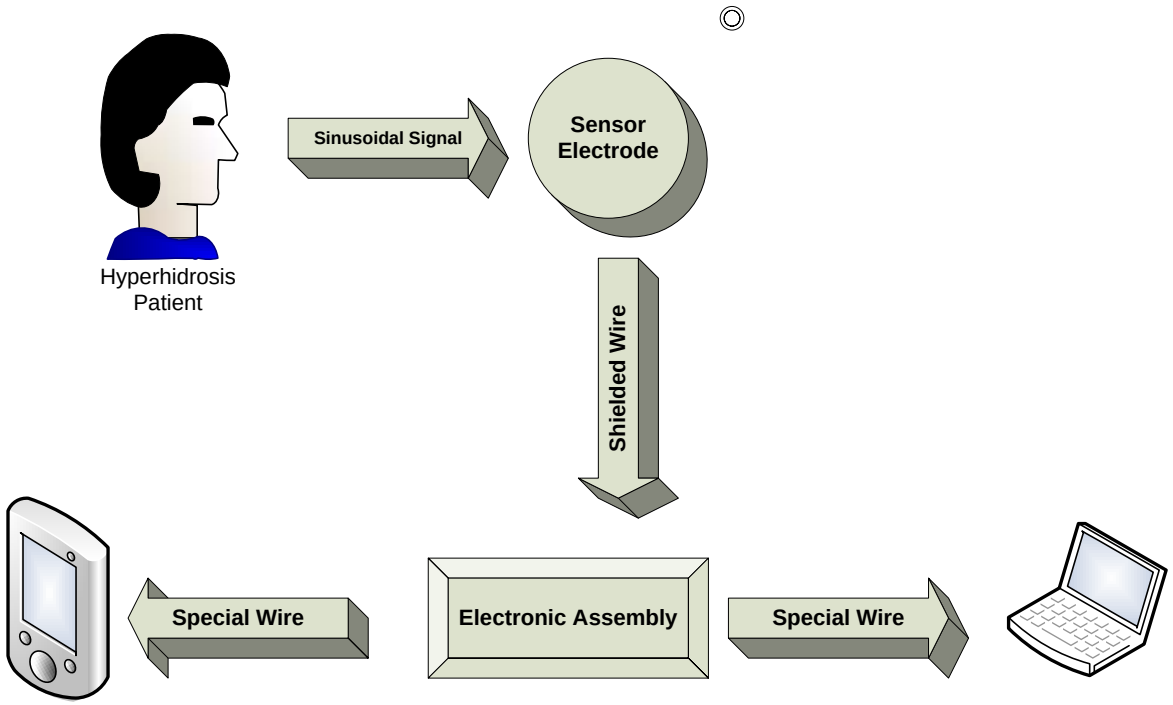

Figure 2: Device Flow Diagram

CHAPTER 4

4 Sensor Design and Material

Several skin surface electrode designs have been studied before designing the new probe. A three electrode system was designed already 1937 by Barnett [22]. A two electrode bipolar system was used by Yamamato et al., the larger electrode 10 times larger area than the smaller electrode [23]. Martinsen et al. introduced a third current carrying electrode within the same geometry in order to reduce deeper tissue interaction affecting series impedance [22].

The above techniques were used to make sensors for measuring skin impedance to some depth into the skin, unlike the present goal. In this work, a geometrical arrangement suitable for detection of a sweat layer on top of the skin was used, i.e. two concentric rings having diameter 10mm and 30mm, respectively. The outer end of the hollow cylinder sensor is open in order not to interfere with the building of a sweat layer. See Figure 3

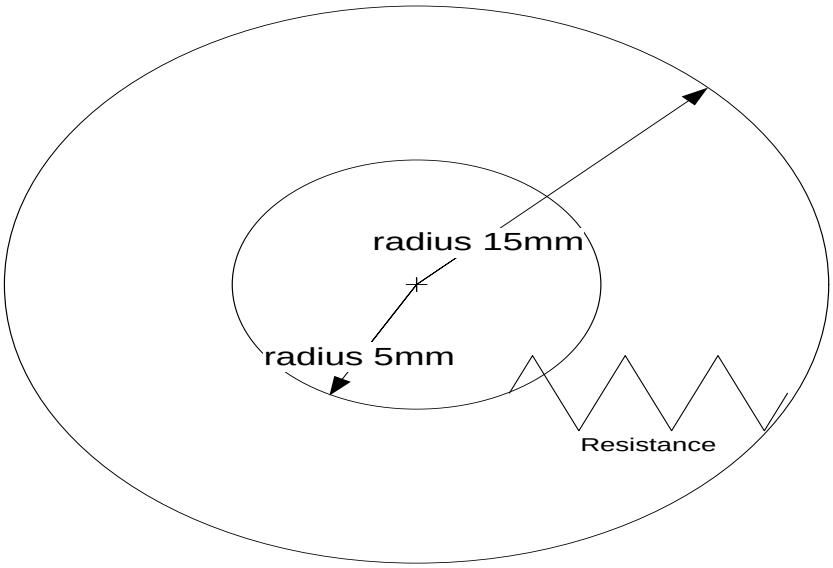

Figure 3: Surface Sensor Dimensions

4.1 Resistance calculations

For a bar or wire, resistance can be calculated as:

$R = \rho L/A$ Eq 1

where ρ is the resistivity, L is the length, and A is the cross-section area.

For sweat, ρ is in the range of 1 Ωm, and this value is used in all approximate calculations of this thesis.

A rough estimate of the expected resistance of the new sensor can be calculated by considering two parallel electrodes of length 2π x 'average radius of the outer and inner rings', 10 mm apart. L in Eq 1 would then be the separation of the electrodes, i.e. 10 mm, and A 2π x 10 mm x h, where h is the height/depth of the sweat pool between the electrodes. Thus, with the given dimensions: R is approx. ρ/2πh [h in meters], see Figure 4.

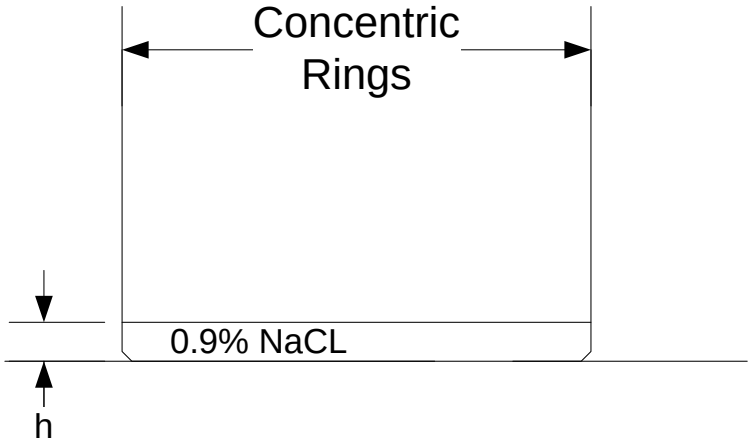

Figure 4: Sweat height estimation

A table with realistic values of R for various values of h is given in Table 2.

Table 2: Resistance Variation with Height of Sweat (with identical electrolytes/ions)

S.No	**Resistance**	**Height of Sweat**
01	100 Ω	1.5 mm
02	200 Ω	795 μm
03	300 Ω	530 μm
04	400 Ω	398 μm

05	500 Ω	318 μm
06	600 Ω	265 μm
07	800 Ω	198 μm
08	900 Ω	177 μm
09	1 kΩ	159 μm
10	10 kΩ	15.9 μm
11	20 kΩ	7.95 μm
12	30 kΩ	5.3 μm
13	40 kΩ	3.9 μm

From Table 2 a rough estimate of the contribution from the sweat pillar (hollow cylinder between the concentric electrodes) can be made. The resistance between the two concentric ring metal electrodes changes inversely with the height of sweat. It means that if there is no sweat on the skin surface, detected resistance will be maximum, and only the natural skin hydration would then contribute to the reading. However, on dry hands the device will be out of range.

4.2 Material Used For Electrode

Brass is the material used for making the concentric ring electrodes in this project.

4.3 Sensor Electrode Probe

The Sensor Probe is an important part of the device, and the actual measurement values will depend on the actual shape and dimension of the electrode system. The electrode system of the present prototype was mounted on a plastic kitchen tool, a frying spade with slits that allow vapour to pass through. This laboratory style solution is cheap, comfortable, and provides easy access to various application areas, and also has light weight. See Figure 5. In the picture can be seen that the sensor has three plastic screws keeping the concentric metallic rings apart with fixed distance. The brass rings have soldering ears attached, providing stable connection to wires. Performance characteristics will be discussed in the next chapter.

Figure 5: Sensor Probe

Two wires connected to the soldering ears carry signal from the dry electrodes to the electronic assembly. In comparison with solid wire, stranded wires have better flexibility and have same total cross sectional area, and should not introduce any measurement error at the used frequency. Stranded wire was chosen for its flexibility [24].

4.4 Electronic Assembly

The analog signal from the probe is then processed and filtered by the electronic assembly and the ensuing signal is entered to the computer sound card or to a SmartPhone. The signal flow is depicted in Figure 6.

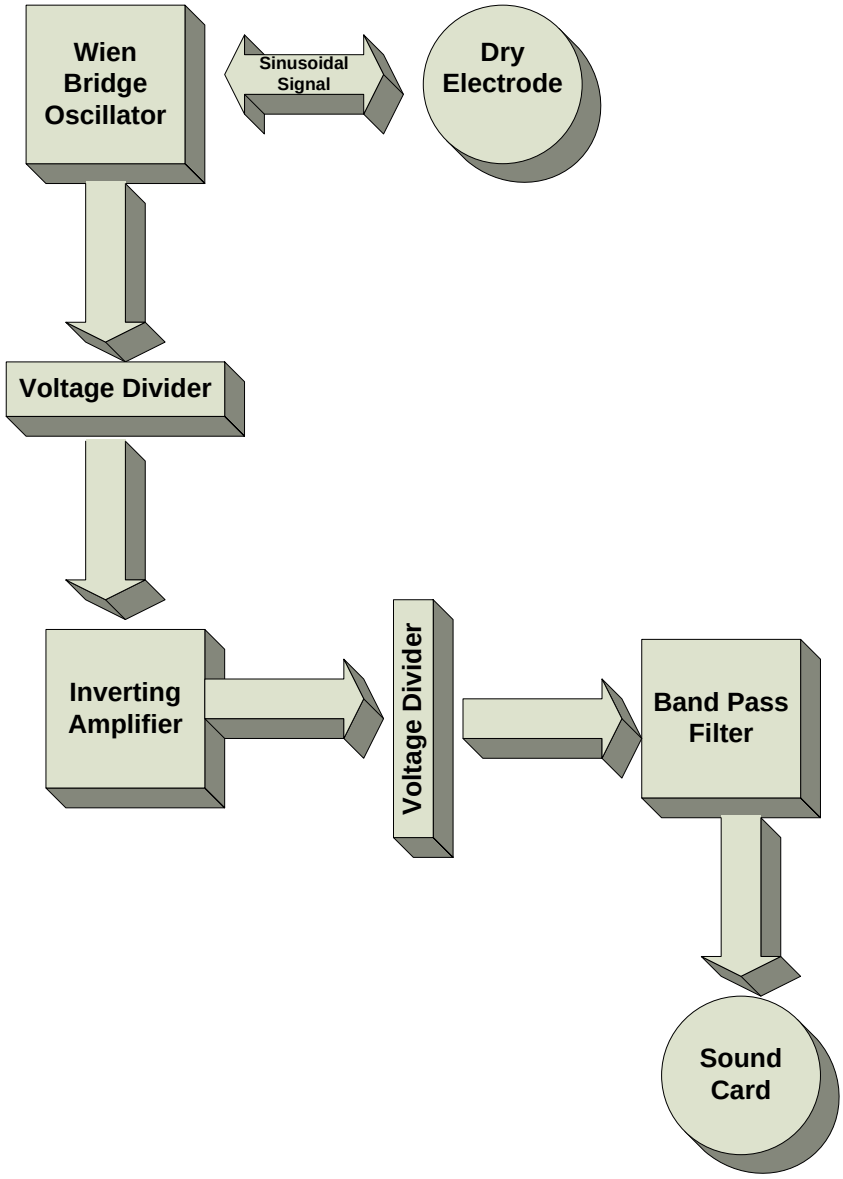

Figure 6: Electronic Assembly Flow Chart

4.4.1 Wien Bridge Oscillator

A Wien Bridge Oscillator is a circuit used for generating low frequencies in typical range of 10 Hz to about 1 MHz. [25]. This device circuit uses three operational amplifiers (Op amp). One for the oscillator, one for the resistance to voltage conversion, and one for a band pass filter. One amplifier stage causes 180 degrees phase shift and a feedback network adds another 180 degrees phase shift to form a 360 phase shift in a loop at the chosen characteristic frequency [26].

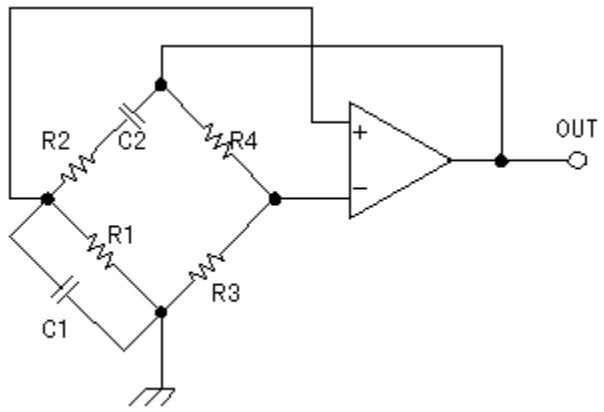

Figure 7: Wien Bridge Oscillator

Resistors R1, R2 and capacitors C1, C2 in figure 7 are the components that control the oscillation frequency of this circuit. R4 and R3 form a feedback network. These resistors control the gain of the non-inverting amplifier circuit [26].

$$A = 1 + R4/R3$$

First we have to satisfy the Barkhausen Criterion $AB \geq 1$, it means the gain of non-inverting amplifier should be minimum 3.

$|A| \geq 3$, thus:

$R4/R3 \geq 2$

Frequency of oscillation is

$f = (1 / 2\pi RC)$ Hz

This formula is valid if R1, R2 and C1, C2 are equal, respectively.

- Wien bridge calculation and circuit diagram is described in Appendix A

4.4.2 Inverting Amplifier

The inverting amplifier is one of the basic configurations of an Op amp. In this configuration the non-inverting input of the Op amp is connected to ground and the signal is applied to the inverting input terminal. Figure 8.

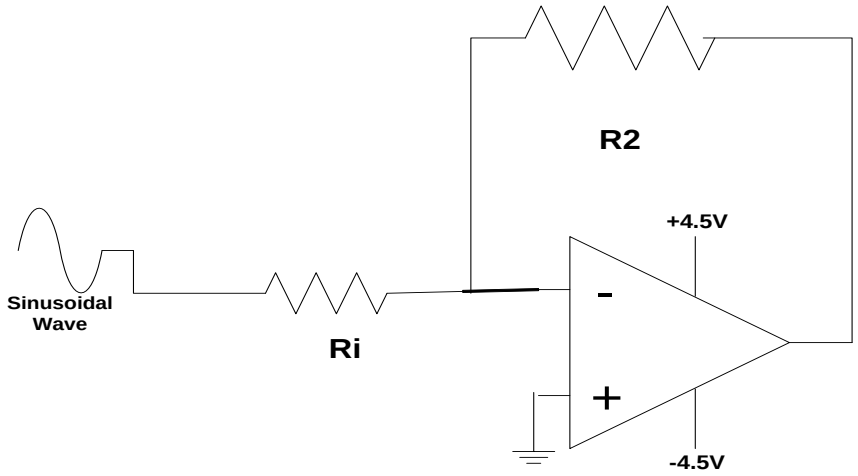

Figure 8: Inverting Amplifier

$A = - R2 / R1$

Negative sign indicates that input and output are out of phase by 180^0 [27]. The gain of Amplifier (A) can be adjusted by the ratio of R2 (feedback resistance) and R1 (input resistance). The system under test, SUT, i.e. the probe attached to skin, replaces R2, so that the actual resistance of this system varies the amplification. In this way, the output voltage will be proportional to the resistance of the system under test, i.e. inversely proportional to the amount of sweat, given the fixed magnitude of the oscillator at the chosen measurement frequency. Thus, variations in the SUT can be easily obtained, as shown in Figure 9.

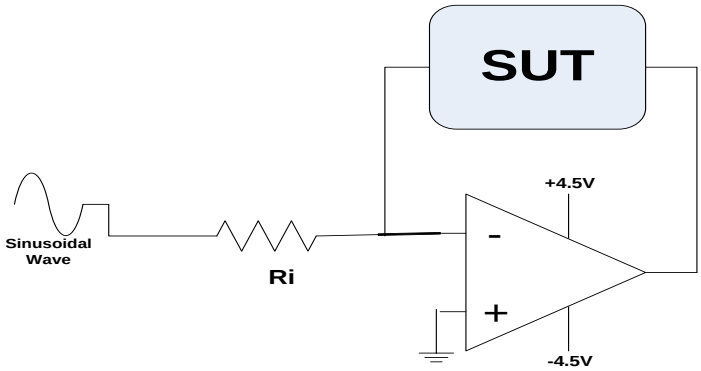

Figure 9: Inverting amplifier with SUT

4.4.3 Power Supply and Voltage Divider

A 9V battery based power supply was arranged to drive the op amps with ± 4.5V, see Figure 10.

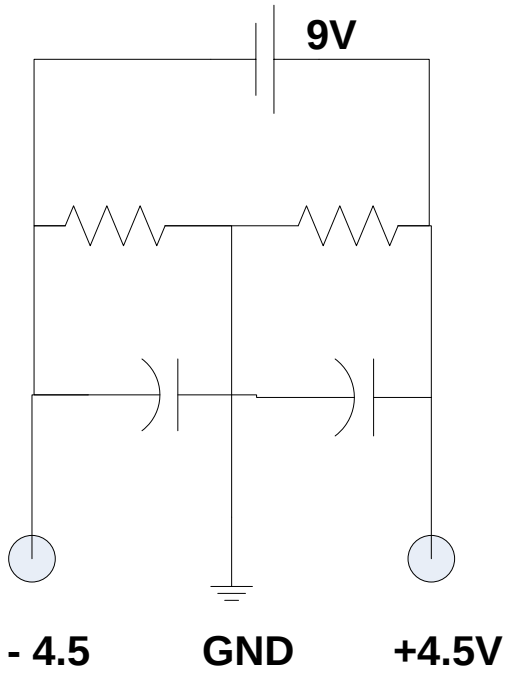

Figure 10: Power Supply Schematic

Voltage divider used in this circuit is to divide the incoming voltage from a 9V battery, providing a virtual ground level in the middle [28].

4.4.4 Band Pass Filter

A band pass filter is used for selecting a particular band of frequency, in this case admitting only the oscillator frequency

On the Basis of Quality Factor (Q) we can classify Band Pass Filters in two types [29]

- Wide Band Filter
- Narrow Band Filter

4.4.4.1 Wide Band Filter

If Quality Factor (Q) < 10, the band pass filter will be Wide Band. It is formed by cascading high pass and low pass filters.

4.4.4.2 Narrow Band Filter

If a more narrow band pass filter is desired, an op amp with two feedback paths can be used, see Figure 11. Due to its feedback network, it is also called Multiple Feedback network [29].

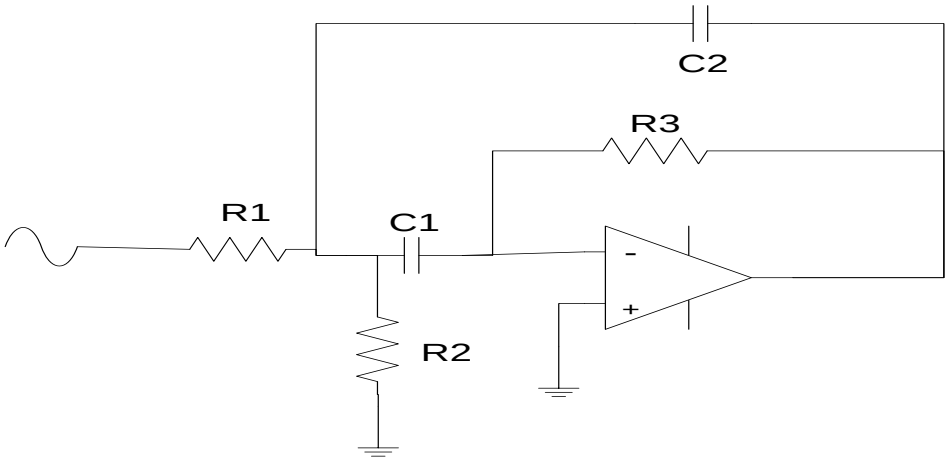

Figure 11: Narrow Band Pass Filter

The important parameters in narrow band pass filters are cutoff frequencies (F_H & F_L), resonant frequency, circuit gain factor, and Quality factor [29]. The relationships between them are as follows:

For Simplicity we choose capacitors C1= C2 = C

$R_1 = Q / (2\pi f_c C A_f)$

$R_2 = Q / 2 \pi f_0 C (2Q^2 - A_f)$

$R_3 = Q / \pi f_c C$

4.5 Sound Card

The Sound card is used as an analog to digital converter, where the analog voltage represents the value of the impedance of the sensor, i.e. inversely represents the sweat level. Creative Sound Blaster live value PCI sound card was used.

Sound Card basic components

1. Digital to Analogue converter (DAC).
2. Analogue to Digital converter (ADC).
3. ISA or PCI slot for interfacing sound card with mother board.
4. Connectors for input and output for sound processing.

The sound card uses CODEC that performs both functions ADC and DAC processing. The sampling rate was set to 44.1 ksamples per second.

Manufacturers use mainly two parameters to describe quality of sound equipment:

- Total Harmonic Distortion
- Signal to Noise Ratio

The Sound card also has a Digital Signal Processor that reduces the work load from the computer during sound processing. It can process multiple channels of sound simultaneously. It also has its own memory for faster processing speed. In this project, the external microphone connector was used to input the analog signal to the computer [30].

4.6 Audio Connectors

There are many types and standards of audio connectors, e.g.

- RCA Connectors
- XLR Connectors
- Phone Connectors
- Microphone Connectors

Microphone connectors were used to make special cables for interfacing with Laptop and SmartPhone.

4.6.1 Microphone Connectors

Microphone connectors are available in different sizes like ¼ inch (6.35mm), 1/8 inch (3.5mm) 3/32 inch (2.5mm) and number of contacts, i.e. two, three or four. Modern connectors are TRS connectors. The letters represent the name of the conductors T (Tip), R (Ring), and S (Sleeve). TRS connectors consist of three conductors as depicted in Figure 12 (A) for Laptop interfacing, and TRRS connector having four conductors shown in Figure 12 (B) for Smartphone interface. The reason behind using these connectors is the female connector requirements of the computer and Smartphone respectively. In the Laptop sound card, there are two different ports for microphone and headset. The signal was sent via the Tip of the connector into the Laptop.

A B

Figure 12 TRS and TRRS Connecters

The Smartphone required a TRRS connector. The signal was sent into the smart phone via Tip, but ring could also have been used. This is the reason they have been called “specialized” cables [31].

CHAPTER 5

5 Sound Card Oscilloscope Software

This software is not a freeware, but is free for private use as well as non-commercial use, as granted by the manufacturer.

5.1 Software Requirement

- Windows XP, Vista, 2000, Windows 7 (64 bit version), Windows 8
- Minimum 50Mb disc space required
- PC having sound card properly installed.

5.2 Software Description

Sound Card Oscilloscope software is usually intended to use for the wave display and measurement of sound waves in the form of frequency and amplitude. The sound wave input can be taken from direct interface of a microphone with the sound card, or it can be taken from Compact Disk (CD) and media player. Software takes sound data via Windows interface from the sound card. User interface is similar to the conventional analogue oscilloscope. The Electronic Sudometer uses a frequency of 294 Hz for measurements and this frequency is within the audio band, so this software or any sound software can be used to calculate and display the signal in the present project.

5.2.1 Main Menu

The Sound Card Oscilloscope has two channels in the software window, as is shown in Figure 13. The left and right channels are distinguished by the green and red coloration. The software has two types of knobs in main menu, i.e. frequency and amplitude. Edge trigger selector is also available, using rising edge or falling edge characteristic.

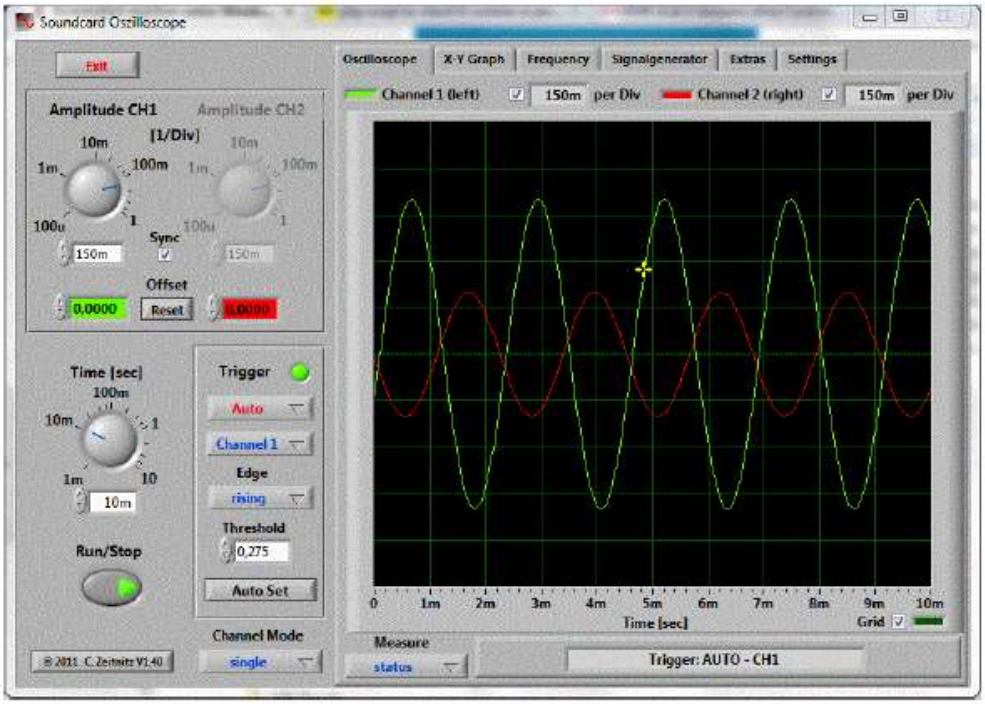

Figure 13: Sound Oscilloscope Main Menu

5.2.2 Amplitude Selection

Amplitude for both channels can be set individually or synchronously. By checking the button called [Sync] one can synchronize the amplitudes of both channels and through Uncheck it is possible to select individual amplitudes, as depicted in Figure 14.

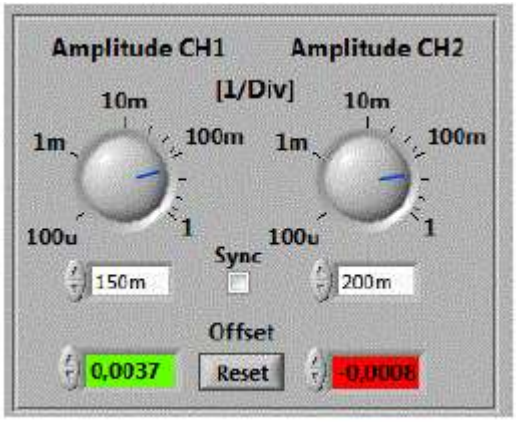

Figure 14: Amplitude Knobs

Amplitude can be set in units per division. Given amplitude values correspond to the level of sound digitization by the number 32768 which represent 16 bit resolution of sound data that were taken from the sound card. Because of different settings of sound volume, absolute sound level cannot be detected directly. Given values thus represent arbitrary units. Offset can be changed individually for each channel. By clicking the fields of offset, two horizontal cursors appear on the software display screen. Offset can be set in two ways, either by entering values in the offset field, or by moving these cursors using the mouse. If no change in offset is made, the cursor will disappear. The offset values can be seen in Figure 15.

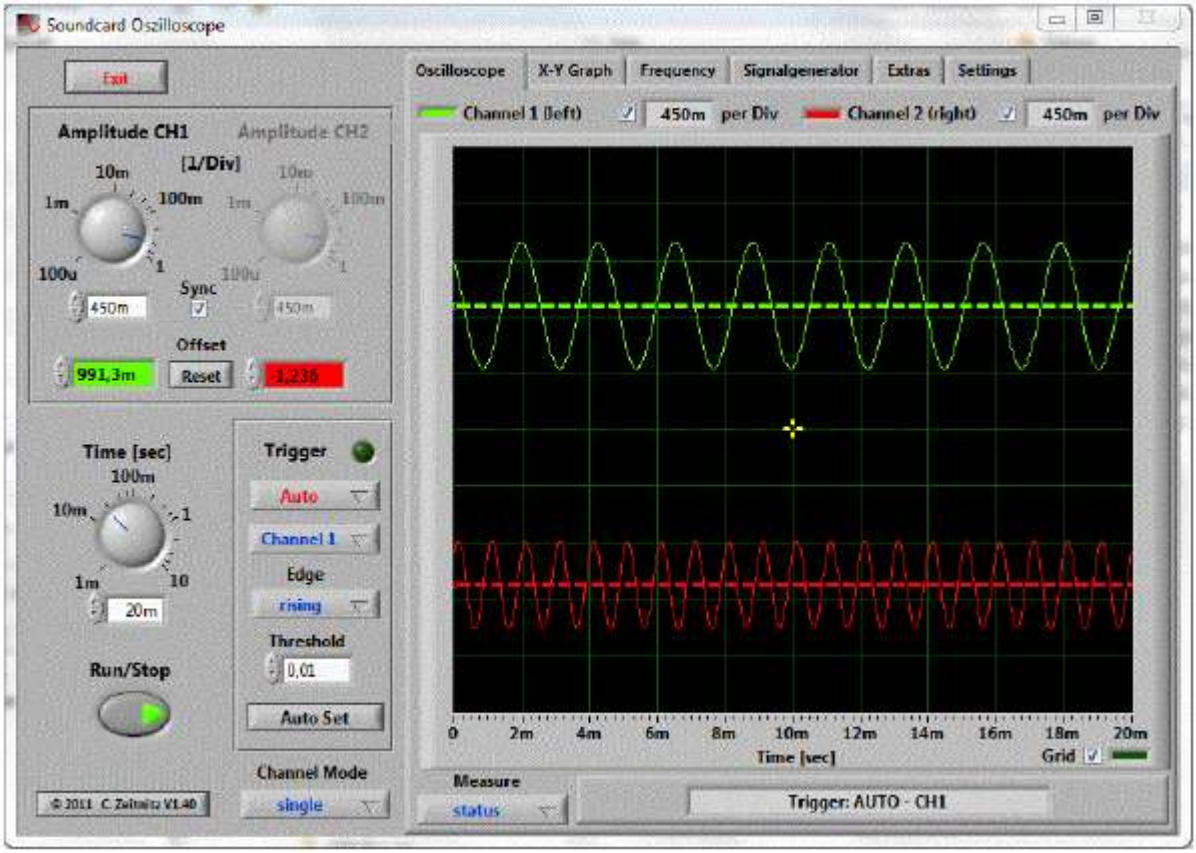

Figure 15: Offset cursor in the middle of Display.

5.2.3 Time Base

The [Time] knob can make the entire range of waves appear on the screen. This function is somewhat different from a normal oscilloscope.

5.2.4 Trigger Function

The trigger menu has four functions “Off, Auto, normal and single”. These are standard modes of normal oscilloscopes. Trigger threshold can be set through the input window or it can be set through moving the yellow cursor present on the screen.

[Auto Set] selection triggers the program to estimate trigger level and time base. The frequency present in the trigger channel helps to get optimal time base. Trigger threshold is relying on amplitude. If the amplitude level is too small, this button would not work. The low level threshold is 20 Hz, below this frequency results are not reliable.

In single shot trigger, [Run/Stop] button is deactivated and has to be pressed again and again for taking new data, e.g. single pulses.

5.2.5 Data Analysis

Before data analysis, the waveform is frozen by pressing the button called [Run/Stop]. The required waveform can be measured in the form of frequency, Peak to peak voltage, and RMS voltage. In this Master thesis project, only single channel measurements are used.

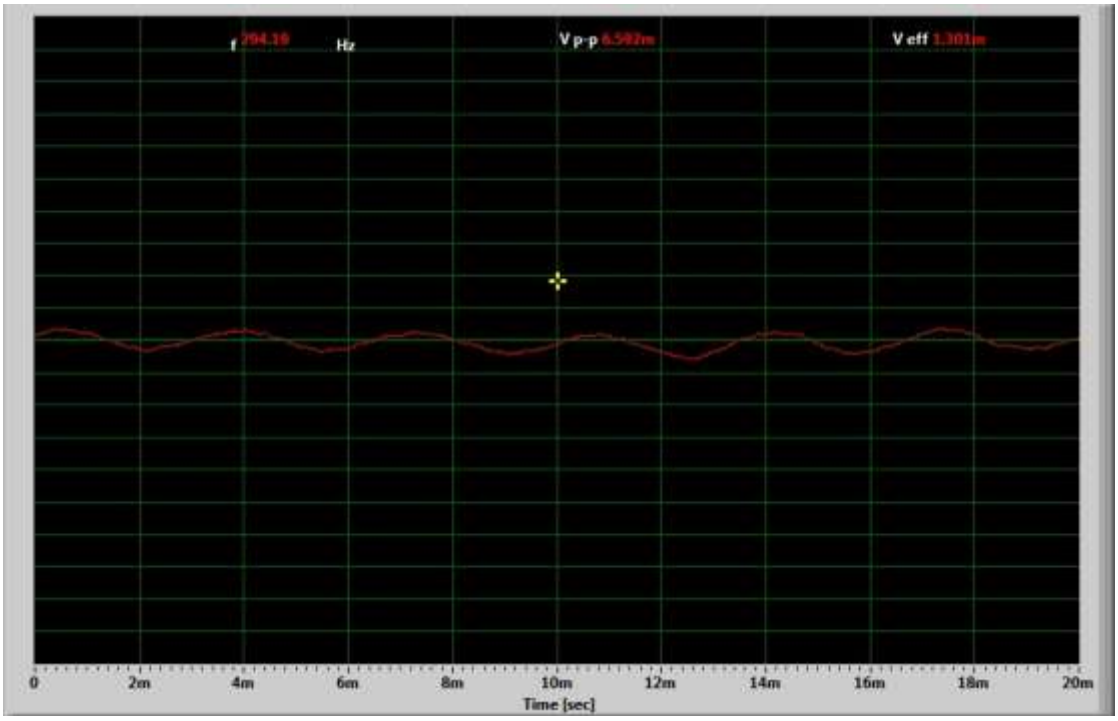

Figure 16: Data Analysis using single channel measurement

5.2.6 Storing Measured Data

The output display can be stored or saved; first data acquisition has to be stopped using the button [Run/Stop]. The save button appears on the software screen after pressing [Run/Stop] button. This option can save the displayed data in the form of a picture in e.g. format BMP, PNG or JPG. An example of a saved image is shown in Figure 16.

5.2.7 Software Calibration

The software can be calibrated by comparing the output voltages with a normal calibrated oscilloscope with displayed voltages. Scope parameters are important to calibrate the software, as depicted in Figure 17. Amplitude calibration is given in V/Div.

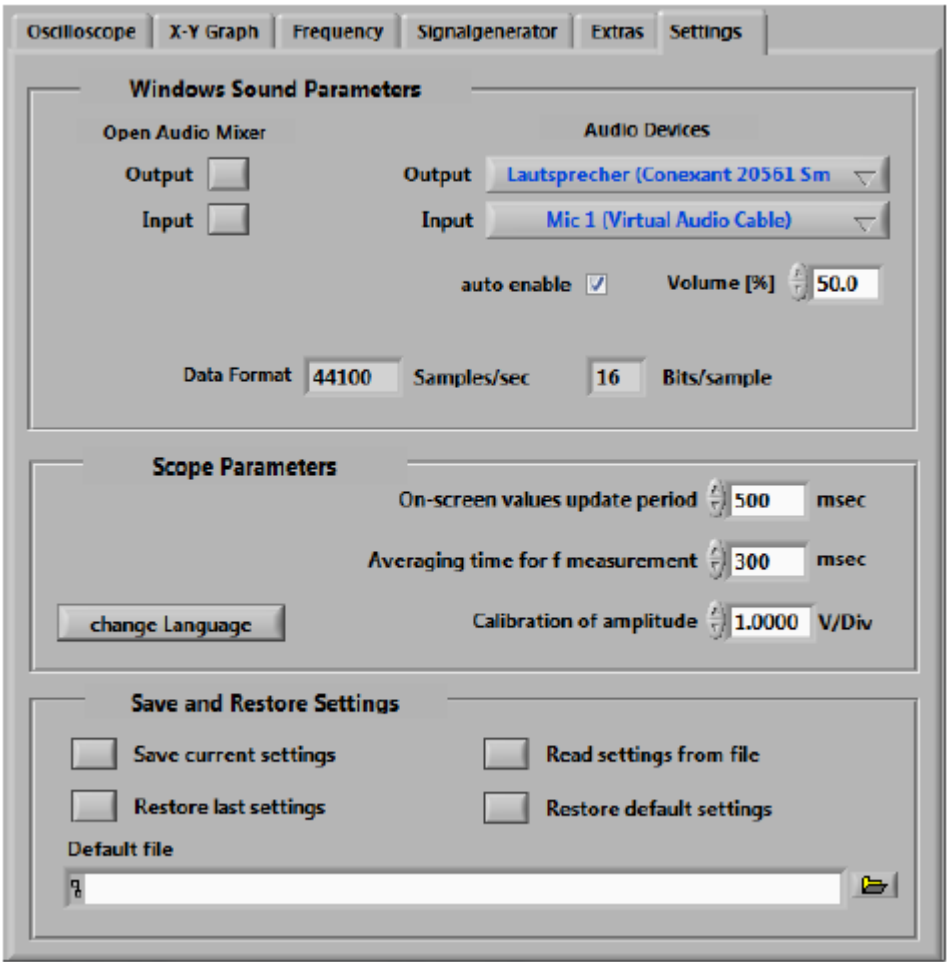

Figure 17: Software settings

This software assumes that the soundcard has 44.1 kHz sampling frequency with 16 bit resolution, which is the case in the soundcard used in this project.

CHAPTER 6

6 Android Application for Soundcard Interface

6.1 Software Description

The intention behind building this software is to make an Android software that can function as a Mobile Oscilloscope. This is an open source oscilloscope software, based on a Bachelor thesis "Using Android in Industrial Automation" from the University of Applied Sciences, Northwestern Switzerland. This software interfaces with hardware using two types of connection: Microphone connection and USB interface. USB connection requires its own hardware. The Electronic Sudometer is connected via the microphone connector. The user interface can be seen in Figure 18.

6.2 Software Features

- Easy to understand user interface
- Two Channel Display.
- Trigger adjustable via mouse or touch screen.
- Audio Source selection (Microphone, USB or Generator).
- Maximum resolution for continuous mode 5 μs/Div
- Minimum resolution for continuous mode 2ms/Div
- 30 frames/s
- Maximum resolution for Single Shot mode 625 ns/Div
- Minimum resolution for Single Shot mode 1.875 μs/Div

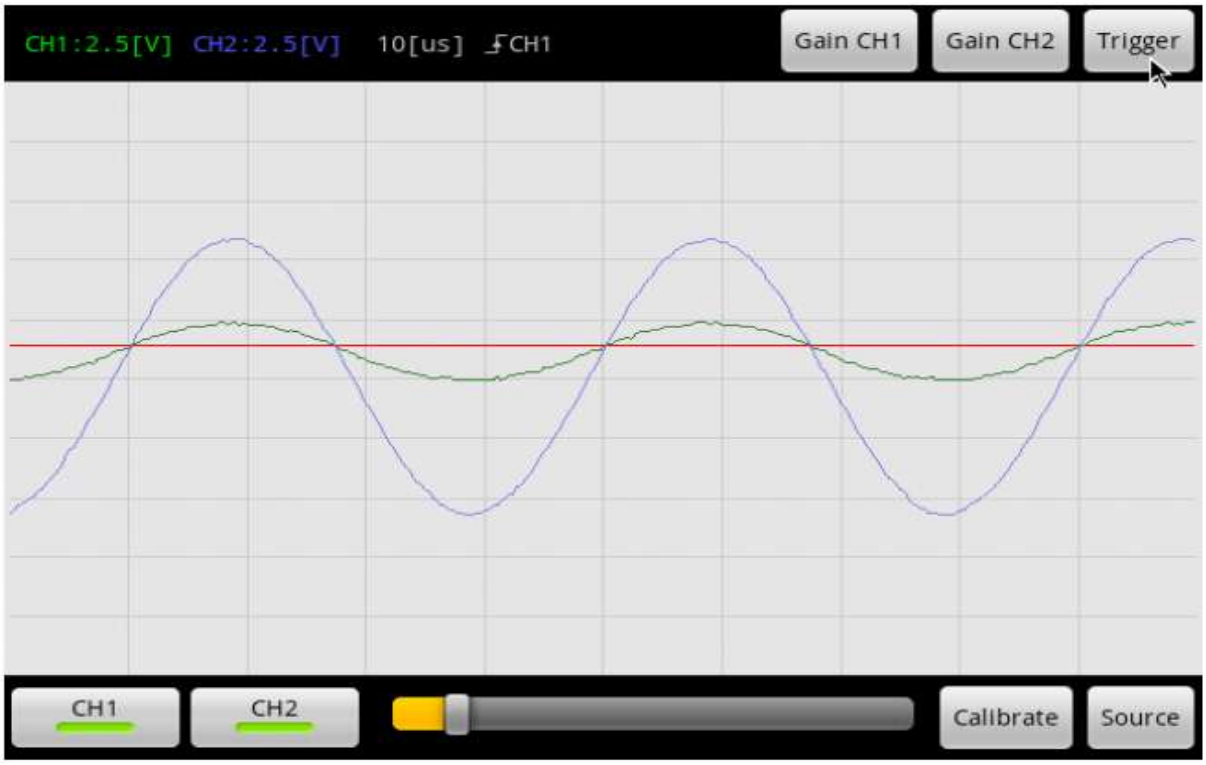

Figure 18: Osciprime Application user interface

6.3 Sample selection and Trigger

An important feature of any oscilloscope is its 'trigger'. The trigger is used to capture certain sets of data points. When the microphone signal output voltage reaches a certain threshold voltage, the trigger is activated. Then, the user can view the area around that predefined trigger point. Through time shift, the user can focus on selected data close or away from the trigger point. In Figure 19 is shown how skipping of data points affects the signal resolution.

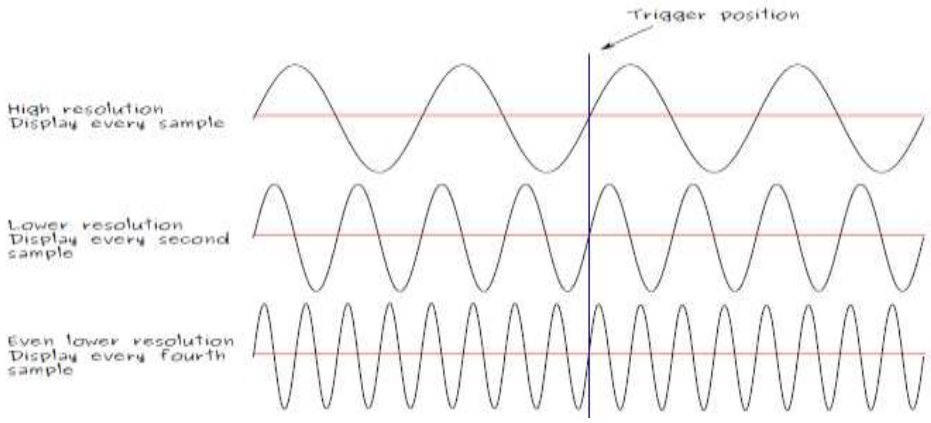

Figure 19: Skipping of data points affects signal resolution

Sample selection during block based data acquisition can be achieved by the following process:

- Find all trigger features that may be present in a block.
- Select the trigger point close to the calculated median index.
- Selection of each and every point within the trigger depends upon time scaling, as depicted in Figure 20.

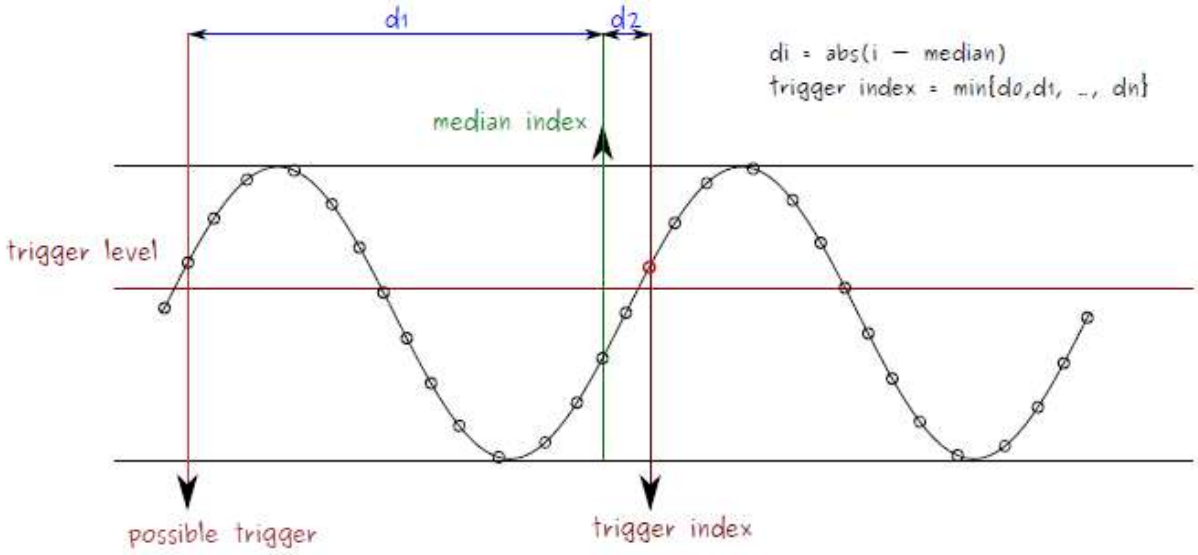

Figure 20 : Selection and detection of trigger.

Assuming that M are samples displayed on the screen, the block length B should be greater or equal to M.

In this application samples are taken with sampling rate 6 ksps in each channel. For 30 frames/s display, 2*B that is 396288 are taken in one frame. So then M = 300 of samples/channel are displayed for the user. Adjustments of sample selection are made depending upon time scale, which is the reason we can vary the display window. Examples of various selections are depicted in Figure 21.

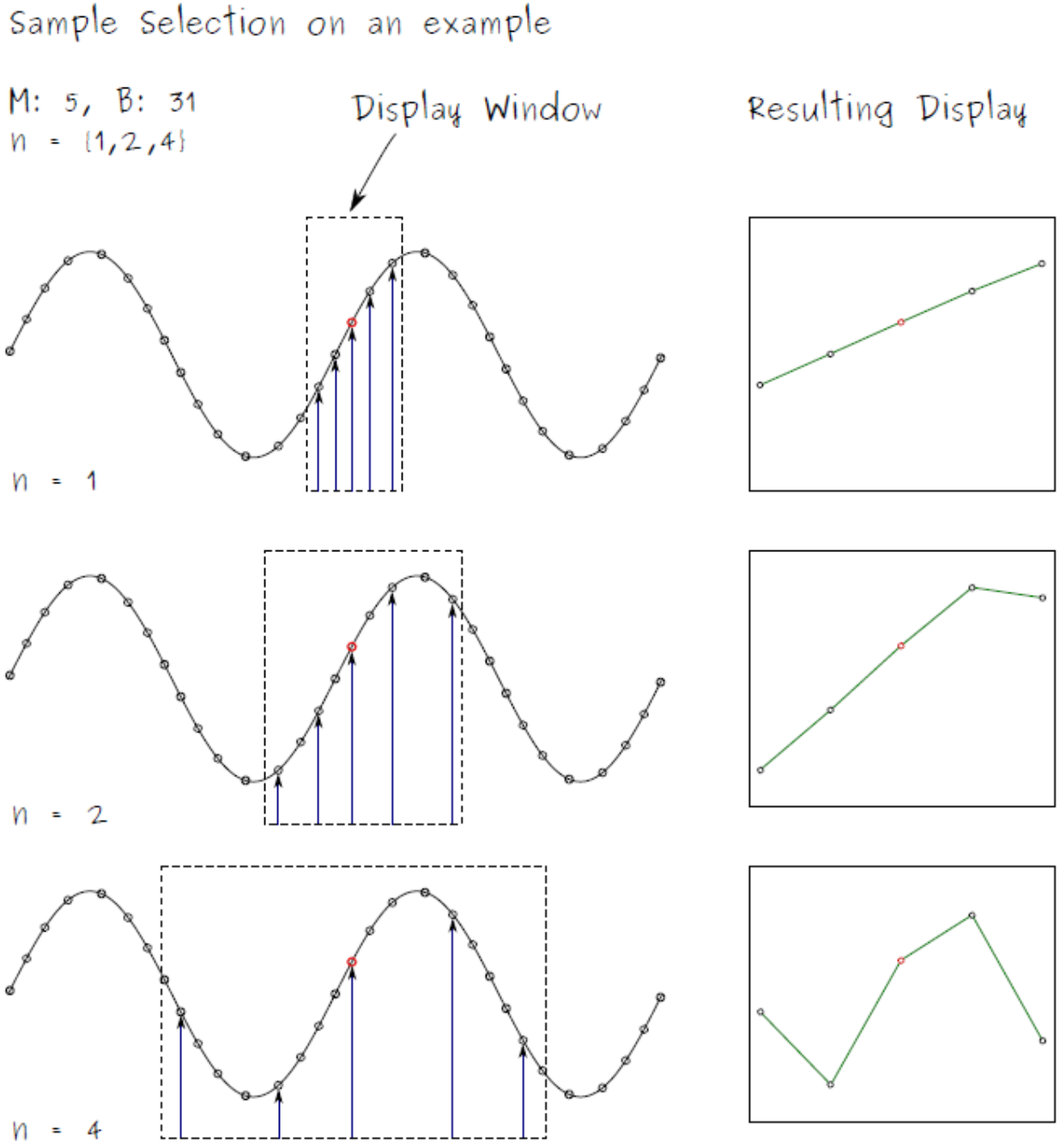

Figure 21: Sample selection examples (sampling intervals should be equal in each case)

CHAPTER 7

7 Experimental Work

7.1 Experiment on Fixed Resistors

7.1.1 Introduction

The device Electronic Sudometer is made for measuring sweat level using electrical impedance measurement. For this purpose, the device has to be calibrated according to known values of resistances to make sure readings are accurate.

7.1.2 Materials and Methods

Fixed resistors declared to be within 1% accuracy was measured to relate the output of the Electronic Sudometer to a known physical reality.

7.1.3 Result

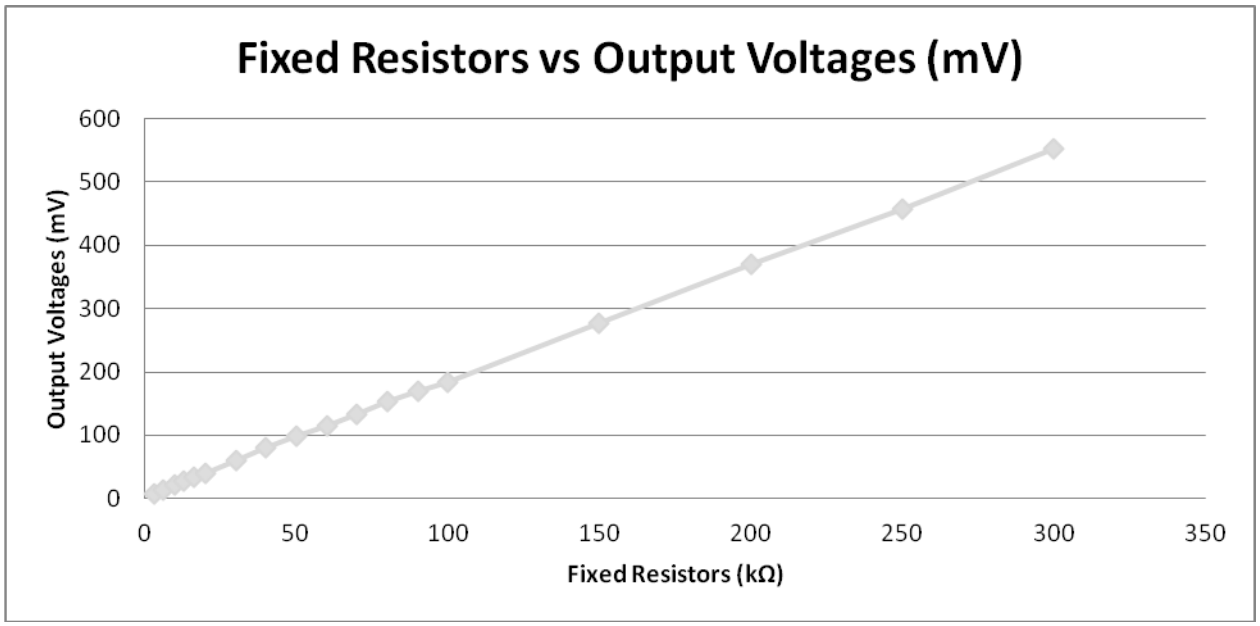

Figure 22: Electronic Sudometer Outut Voltages vs. Fixed resistors

The output of the Electronic Sudometer for different fixed resistors is depicted in Figure 22. It shows the linearity of the device.

7.2 Experiments with an “artificial skin model” (Wettex cloth) inundated with Saline Solution

7.2.1 Introduction

The living strata of human skin have high level of water content and during sweating the water level present on the surface of the skin is increased, especially in HH. In order to understand the relationship of water level with EBI, WTX cloth, as depicted in Figure 23, was used as an “artificial skin model”. Saline solution was added to monitor the impedance at different levels of “physiological” water content.

Figure 23: Wettex Cloth

7.2.2 Materials and Methods

7.2.2.1 Experimental setup

Various amounts of physiological saline solution were added. WTX, a spongy cloth, consists of 35% cotton and 65% cellulose. For weighing of WTX sample along with a plastic bag, a Sartorius balance (TE1535- DS) was used, Figure 24(A). For reasonable accuracy in sample inundation, a pipette as shown in Figure 24(B) was used.

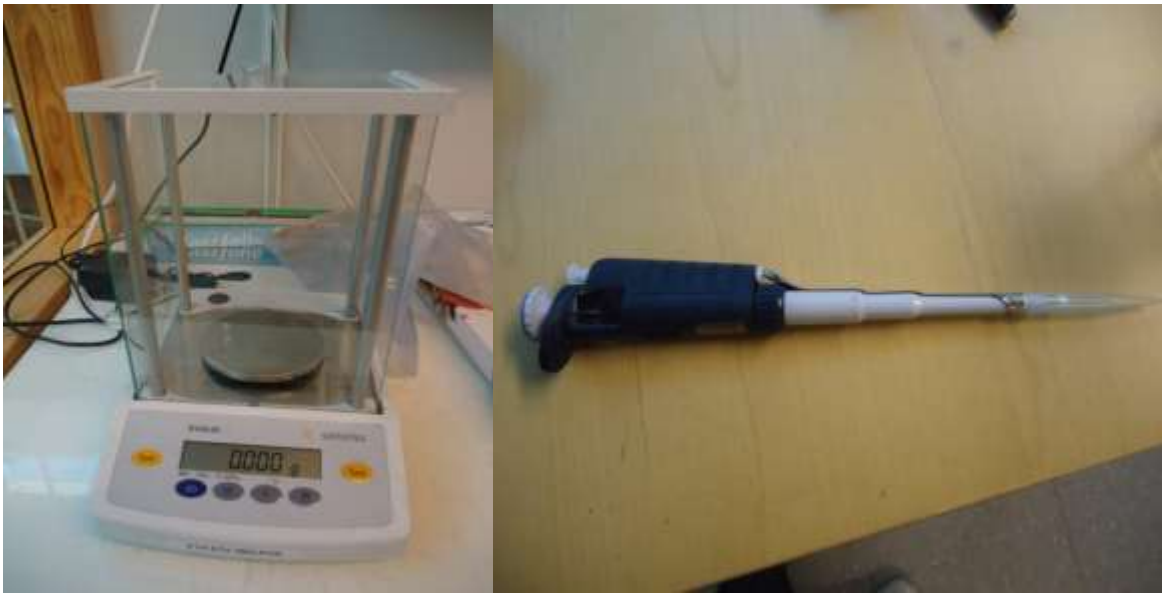

(A) (B)

Figure 24: (A) Sartorius Balance for sample measurements, (B) Pipette for sample measurements

7.2.2.2 Experimental Procedure

WTX cloth having dimension 17 x 20 cm was cut to 4 equal pieces, i.e. each piece 8.5 x 10 cm. One reason for choosing WTX is its absorbance capability. A piece of WTX along with a plastic bag was weighed, see Table 3. Plastic over the WTX is to prevent from evaporation during experiment. The TARE button on the Sartorius scale was used to save this original dry weight. Known amounts of saline solution were added to different samples. Wetted sample weights and quantities given by pipette are listed in Table 3. Time for spreading of moist in the WTX samples was also controlled. Two hours were allowed for spreading of moist in the samples. Samples in their plastic bags are depicted in Figure 25.

7.2.3 Results & Discussion

The data samples presented in Table 3 are given graphically in Figure 26. This graph shows the clear and monotonous variation in the output voltages of the Electronic Sudometer with increasing level of saline solution, but it is not linear. This drop in voltages is due to the decrease in electrical impedance. Two hours equilibration time was allowed to facilitate homogeneous spread of saline within the WTX sample. The real time output of the Electronic Sudometer is shown in Figure 27.

Figure 25: Wet samples marked with time and weight in their plastic bags.

Table 3: Data representation of Saline in WTX vs. Sudometer output Voltages

Time	Plastic bag+WTX Weight (gram)	Saline Weight (gram)	Sudometer Output Voltage (mV)
5:25	4.165	0.094	27.8
5:30	3.920	0.080	33.6
5:35	3.994	0.078	34.6
5:40	4.204	0.070	40.7
5:47	3.917	0.050	60.9
5:54	4.047	0.045	99.8
5:57	3.876	0.035	162.6

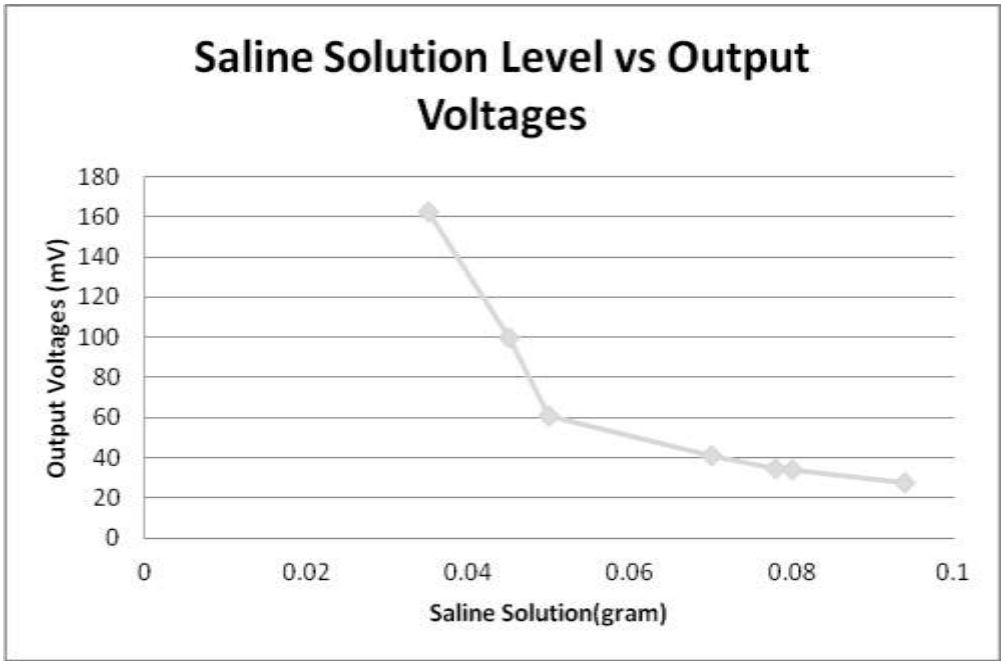

Figure 26: Variation of Output Voltages with amount of saline solution.

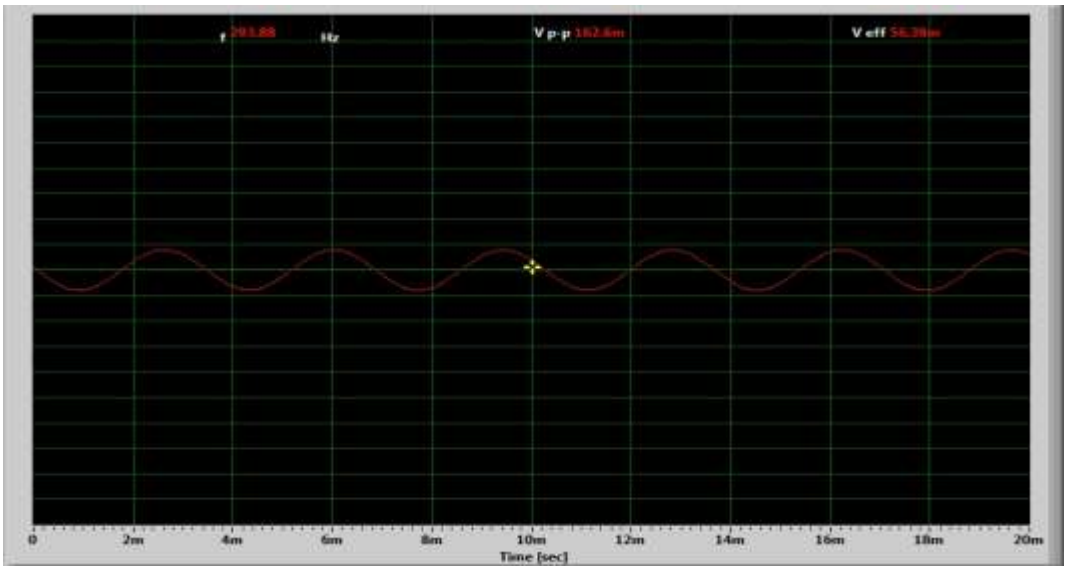

Figure 27: Electronic Sudometer output voltage with 0.035g sample of saline solution.

As mentioned earlier, Table 3 represents large variations in the output voltage corresponding to the saline solution level in WTX. This variation in voltages shows that the device works in the given

range of saline level. In Table 3, liquid samples in the range 30μL to 100μL added to the WTX pieces were used. Before this experiment, 11 readings at high moisture had been tried, see Table 4. The range of pipette samples in Table 4 is from 2mL to 10mL. In this range of wetting, the Electronic Sudometer doesn't provide accurate readings. Large fluctuations in output voltages were seen at this level of wetting with saline solution.

Table 4: Data representation of Saline vs. averaged Sudometer output Voltages

Time	Plastic Bag + WTX Weight(gram)	Saline Weight (gram)	Sudometer Output Voltages(mV)
7:37	4.522	8.71	7.4
7:44	4.350	9.10	4.5
7:49	4.838	7.80	5.6
8:58	4.334	6.89	8.5
8:05	4.496	8.30	6.9
8:12	4.394	7.18	5.3
8:18	4.393	6.30	5.2
8:21	4.465	5.40	6.7
8:28	4.463	3.68	6.2
8:33	4.318	4.60	6.5

7.3 Experiment on Yeast

7.3.1 Introduction

Before application on humans, the device was also tried on non-human living cells, i.e. bakery yeast.

7.3.2 Materials and Methods

For application on living cells, neither human nor animal, yeast was chosen. It is a unicellular fungus. A cube of bakery yeast was used for this experiment.

7.3.3 Result

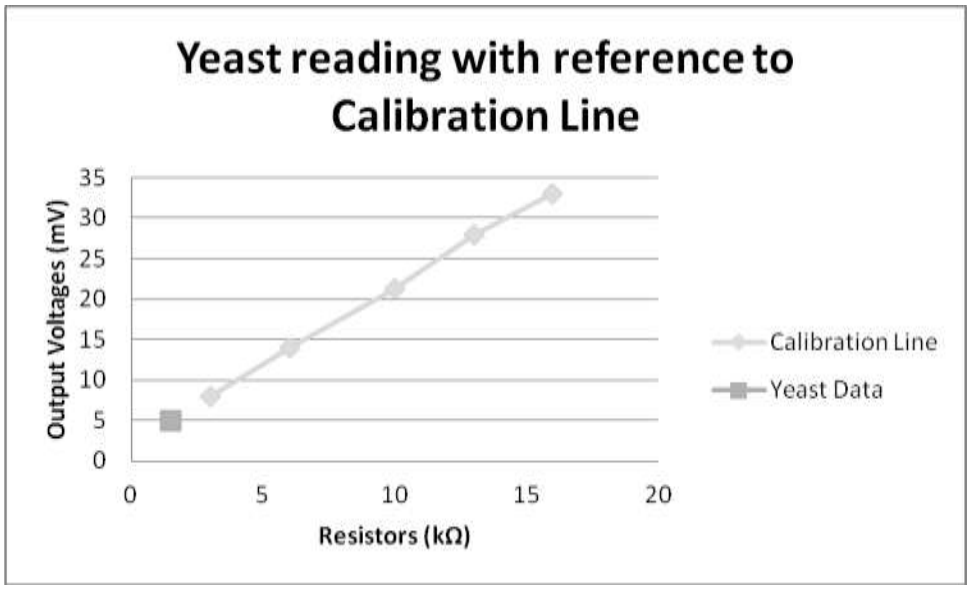

Figure 28: Yeast reading related to the calibration curve.

Figure 28 represents output voltages with respect to the impedance level. The impedance level was about 1.5kΩ, as shown in Figure 28. Obviously, the saline content of yeast culture is higher than the saline content used for calibration, which is consistent with the "singular cell structure" composition contrary to the composition of an organ such as skin.

CHAPTER 8

8 Application on test persons

8.1 Case 1

In this experiment, the author applied the Electronic Sudometer on himself. The author is a healthy individual except that he has HH. Environmental factors are unavoidable. Air humidity of the room was not measured. Theoretically, a serious fault in the computer could have placed the electrodes at 230V although the device itself is battery operated. As an electronics engineer, the author deemed the risk negligible in this prototyping context and since the probe was manually applied to the center of the left hand palm as depicted in Figure 29, the worst case would have been a burn in the palm and that the probe would have been dropped on the floor. No adverse event occurred, but of course this issue has to be solved according to MDD before using on patients.

Figure 29: Author trying Electronic Sudometer

8.2 Result

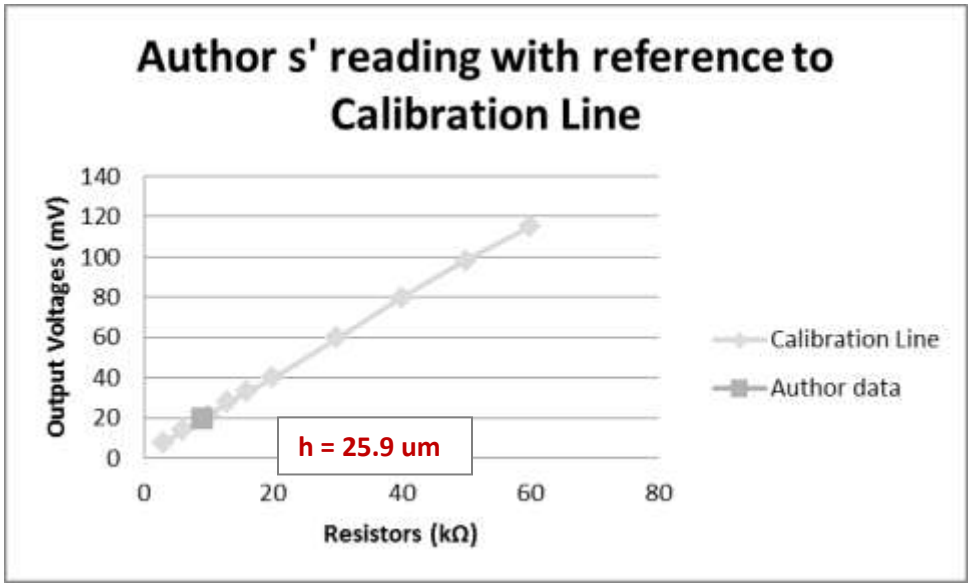

Figure 30: Authors' Electronic Sudometer reading

Figure 30 represents the authors own reading at one occasion when he put the device on his palm. The graph impedance level according to the output voltages is 9kΩ, which is within the expected and calibrated range of values. It is not straightforward to convert the reading to amount of saline on the skin surface, because the skin surface is quite different from the homogenous WTX cloth, even after normalization to size of WTX samples. Probably "arbitrary units" would suffice, and one may as well use the output in mV directly. Theoretically, the height of the saline cylinder defined by the sensor electrodes could be calculated (see General Discussion) however, in this study variation of sweat composition was not included but simply assumed to have resistivity of 1Ωm.

8.3 Case 2

This Master thesis is presented as a work of technology, and no clinical patients were included. However, an engineering student friend with more than normal amounts of sweat in his hands volunteered. Before device application, it was checked that the volunteer had no fever that might affect readings. Environmental humidity couldn't be checked due to the unavailability of adequate instrumentation. The volunteer did not feel elevated temperature in the room. The volunteer applied the device to the center of his palm for the recording of the reading. The volunteer with the Electronic Sudometer probe is depicted in Figure 31. As in Case 1, also this engineer volunteer deemed the risk negligible, and no adverse event occurred during this experiment

Figure 31: Test person trying the Electronic Sudometer Probe

8.4 Result

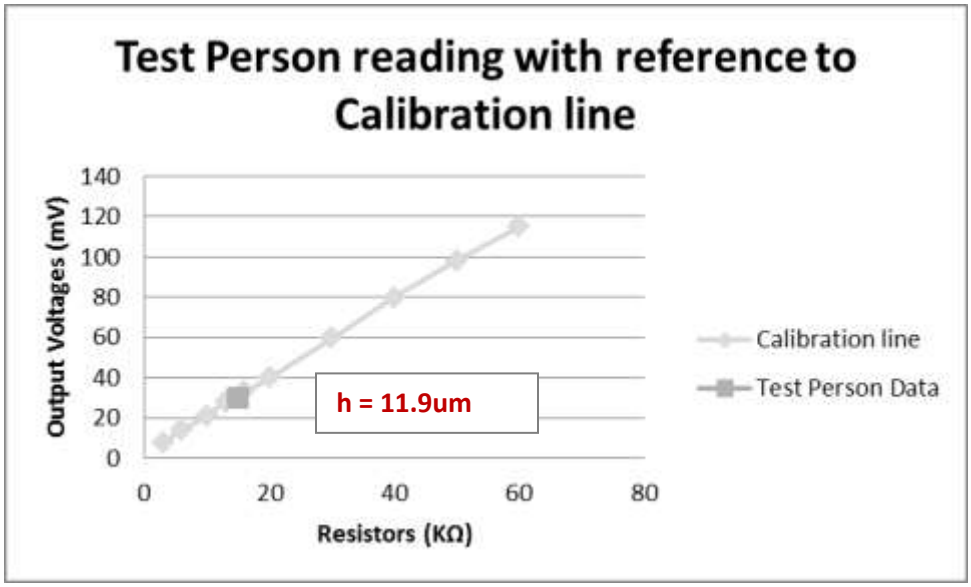

Figure 32: Test person's impedance level related to output voltage

Figure 32 represents the patient's impedance related to the Electronic Sudometer calibration line.

CHAPTER 9

Final Result

The initial phase in the quest for a sweat level measurement device in HH started with possible calibration. Thus, the device was named ***Electronic Sudometer*** and has been calibrated by relating its output voltages to various fixed resistors, as depicted graphically in Figure 22.

To explore possible ranges of sweat level measurements, experiments were performed on inundated WTX considered as a rudimentary "artificial skin model" that could absorb physiological saline solution in various amounts. The moist level was represented as voltages, as shown in Figure 26. There is a clear and monotonous relation between amount of isotonic saline solution and voltage output of the device.

For the purpose to validate the results of the Electronic Sudometer on living cells, bakery yeast was chosen. It has a relatively high amount of water (saline) content, which places it outside the calibrated range, see Figure 28.

After testing on physical and non-animal objects, the Electronic Sudometer was tried on two test persons. In the first case, the author applied the Electronic Sudometer on himself and a recorded reading is shown in Figure 30. The graph represents a comparison of the author's hand reading at one occasion with the calibration line. The low level of impedance indicates high amount of sweat present. (**h**) represents the corresponding height/thickness of sweat layer on the author's palm, according to model assumptions.

In the second case, the device was tried on another test person and the result is depicted in Figure 32. It also shows low level of impedance, but higher than on the author, which shows that the sweat level present on this test person's hand is lower than that of the author's using the simple model of constant resistivity. (**h**) is thus calculated assuming sweat resistivity of 1Ωm for both test persons.

CHAPTER 10

General Discussion

The experiments performed on different objects show correlation between amount of saline hydration and electrical impedance. Despite shortage of volunteers having HH, it is believed that the experiments on WTX cloth and yeast and two volunteers are enough to say that this device can be used to estimate the level of sweat in HH patients.

The experiments on fixed resistors gave a calibration line indicating that the device output voltage is linearly proportional to the electrical impedance.

WTX cloth inundated with saline solution served as a rudimentary artificial skin model, see Table 3. The corresponding graph, Figure 26, shows a monotonous but not linear relationship between amount of saline and voltage output. The non-linearity can be explained by contact artifacts between the WTX cloth and probe electrodes, and varying current trajectories in the relatively thin WTX cloth, which is not easy, if at all possible, to calculate.

Bakery yeast was tried as a live tissue model because it is composed of living cells. It has relatively high water content, and falls outside the calibration curve, Figure 28. Although yeast is a good tissue model, it is not representative of human skin with its layers of different properties. In particular, human skin has the *SC* layer with its characteristic very high impedance at low frequencies. Indeed, at the low frequency used for the Electronic Sudometer, the impedance of the *SC* is at least two orders of magnitude higher than living tissue – even in the wet state [32]. This fact makes it reasonable to assume that, except for the normal impedance level of the *SC* in its natural state of hydration – even if wetted with saline solution, as in reference [32], or by sweat – essentially all of the test current will pass through the hollow cylinder of saline located between the two concentric ring electrodes on top of the *SC*. However, at very low sweat levels, this cylinder is ill defined due to the furrowness of the skin surface, but the inverse of the output voltage would still be monotonously proportional to the amount of sweat.

Cases 1 and 2, which are volunteers featuring HH properties, show that the target of designing a sweat meter has been reached, and the overall results look promising. For research purposes, the experimental Electronic Sudometer could be used with laptop computer or Smart Phone as it is, as long as the system is totally disconnected from mains 230V during measurements. For a commercial product, more design and testing is needed, and the device has to meet requirements according to the MDD. Before clinical testing, ethical permit would be required. Since salinity of sweat may vary over time and between individuals, an additional sensor for sweat composition should be added.

CHAPTER 11

Conclusion

The experiments conducted using the Electronic Sudometer show that this device has capability to measure sweat level in HH. Though it has only been tried on palmar regions, it is believed that it would work on any surface accessible with the probe. After industrial design, including a sweat composition sensor, and more testing, it could become a clinical support tool to monitor efficacy of treatments as well as quantifying severity of hyperhidrosis.

References

1. Baker CR, Reese G, Teo JH, *Rapid Surgery*, Wiley-Blackwell, Sec. Ed. 2010, p. 29
2. Rao DK, Kaur JJ, *New living science Biology for Class 9*, Ratna Sagar, rev. ed. 2009, p.174
3. Harth W, Gieler U, Kusnir D, Tausk FA, *Clinical Management in Psycho Dermatology*, Springer, 2009, p.102
4. "Health Guide." *The New York Times*, (March 19 2013).
5. Hornberger J, Grimes K et al. "Recognition, diagnosis and treatment of primary focal hyperhidrosis." *J Am Acad Dermatol* , vol.51, pp. 274-86, Aug. 2004.
6. Adar R, Kurchin A, Zweig A, Mozes M. "Palmar hyperhidrosis and its surgical treatment: a report of 100 cases." *Annals of Surgery*, vol.186, pp. 34-41, Jul. 1977.
7. Strutton DR, Kowalski JW, Glaser DA, Stang PE. "US prevalence of hyperhidrosis and impact on individuals with axillary hyperhidrosis: Results from a national survey." *J Am Acad Dermatol*, vol.51, pp. 241-8, Aug. 2004.
8. Strutton D, Kowalski J, Glaser D, Stang D. "Impact of hyperhidrosis on daily life and leisure activities in the US for individuals with auxiliary hyperhidrosis: results from a national consumer panel.", Scientific Poster, *Am Acad Dematol Meeting*, 2003
9. Amir M, Arish A, Weinstein Y, Pfeffer M, Levy Y. "Impairment in quality of life among patients seeking surgery for hyperhidrosis (excessive sweating): preliminary results."*Isr J Psychiatry Relat Sci*, vol.37, pp. 25-31, 2000.
10. Hölzle E. "Pathophysiology of sweating."*Curr Probl Dermatol* ,vol.30, pp.10-22, 2002.
11. Kathani A. Amin, MD , "Primary Focal Hyperhidrosis." *DermatologyReview.com Journal*, p. 3, February 2007.
12. Hund M, Kinkelin I, Naumann M, et al. "Definition of axillary hyperhidrosis by gravimetric assessment." *Arch Dermatol*, vol.138, pp. 539-41, Apr 2002.
13. Maillard H, Bara C. "Hyperhidrosis and hypohidrosis." Internet: http://www.therapeutique-dermatologique.org/spip.php?article1549, [1 Feb 2013].
14. Berardesca E, "EEMCO guidance for the assessment of stratum corneum hydration: electrical methods*." Skin Res Technol*, vol.3, 126-132, 1997.
15. Blickmann CW, Serup J, "Reproducibility and variability of transepidermal water loss measurement: studies on the Servomed Evaporimeter." *Acta Derm Venereol*, vol.67, pp. 206-210, 1987.
16. Nicander I, "Electrical impedance related to experimentally induced changes of human skin and oral mucosa." (PhD-thesis) Karolinska Institutet, Stockholm 1998.
17. du Plessis J, Stefaniak A, Eloff F, et al., "International guidelines for the in vivo assessment of skin properties in non-clinical settings: Part 2. Transepidermal water loss and skin hydration." *Skin Res Technol* , vol.19, pp. 265-278, 2013.
18. Mosler K, "Hautfeuchtigkeitsmessung – kein Problem mit dem Corneometer CM 420." *Parfümerie und Kosmetik*, vol.64, pp. 375-379, 1983.
19. Blickman CW, Serup J. "Assesment of Skin Moisture. Measurement of electrical conductance, capacitance and transepidermal water loss." *Acta Derm Venereol*, vol.68, pp. 284-290, 1988.

20. M.H Lader and J D Montagu, “The Psycho Galvanic Reflex: A Pharmacological Study of the Peripheral Mechanism.” *J Neurol Neurosurg Psychiatry*,1962, pp. 126-133.
21. Psykologisk-pedagogisk uppslagsbok. Natur och Kultur, Stockholm 1956, p. 822 (in Swedish).
22. Grimnes S, Martinsen OG, Bioimpedance and Bioelectricity Basics, Second Edition, Academic Press, 2008.
23. Yamamoto Y, Yamamoto T, Ozawa T, “Charactersitics of skin admittance for dry electrodes and the measurement of skin moisturization.” *Med Biol Eng Comput*, 1986, pp. 71-77.
24. Herrick RJ, “DC/AC Circuits and Electronics: Principles & Application.” USA, Delmar , 2003, p. 153.
25. Bhargava NN, Kulshreshtha DC, Gupta SC, “Basic Electronics and Linear Circuits.”, Delhi, Tata Mc GrawHill, reprint 2006, pp. 414 & 423.
26. Bakshi UA, Godse AP, “Linear Integrated Circuits”, Pune. India, 4th edition, Technical Publication, 2009, pp. 76-81.
27. Cox JF, “Fundamentals of Linear Electronics: Integrated and Discrete Circuitry.” USA, Delmar, 2nd Edition, 2002, pp. 325-326.
28. Carter B, “Op Amps for Everyone.” USA, Elsevier, Fourth edition, 2013, p. 9.
29. Bakshi UA, Godse AP, “Analog and Digital IC – Design and Application.” Pune. India, First Edition, Technical Publication, 2009, pp. 111-113
30. Lars Ahlzen, Clarence Song, “The Sound Blaster Live! Book.”USA, No Starch press, 2013, p. 6.
31. Sauls SJ, Stark CA, “Audio Production Worktext”, Focal Press, Seventh Edition, 2013
32. Ollmar S, Nicander I. “Within and beyond the skin barrier as seen by electrical impedance,” In *Bioengineering of the Skin: Water and the Stratum Corneum*, 2nd edition. Fluhr J, Maibach H, Berardesca E, Elsner P (eds.). Boca Raton Fla: CRC Press 2005: pp. 335-350.

Appendix A

Wien Bridge Oscillator

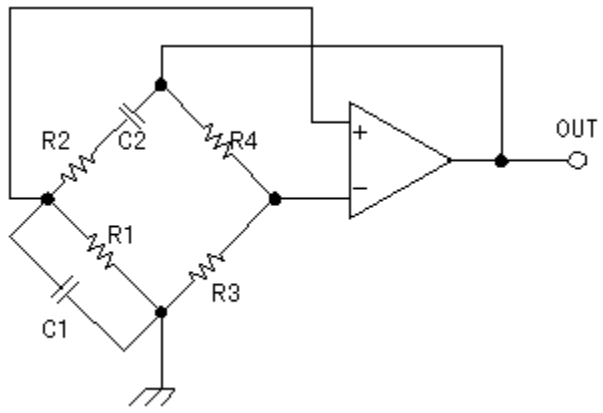

Components

R1 =R2= 1.2kΩ

R 4 = 2kΩ

R3 = 1kΩ

C1 = C2 = 0.47µF

Inverting Amplifier

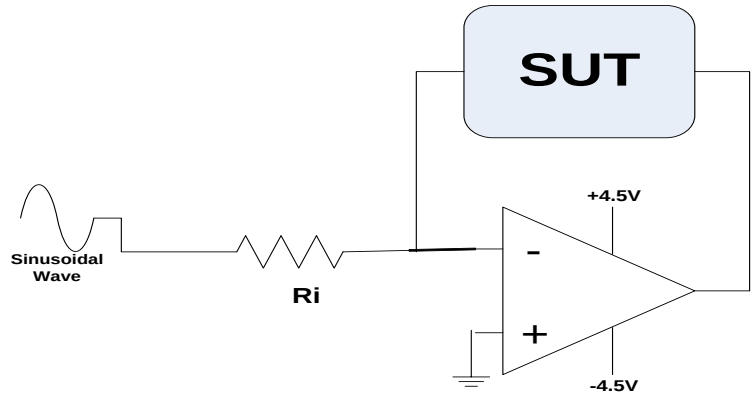

Ri = 1 kΩ

Narrow Band Filter

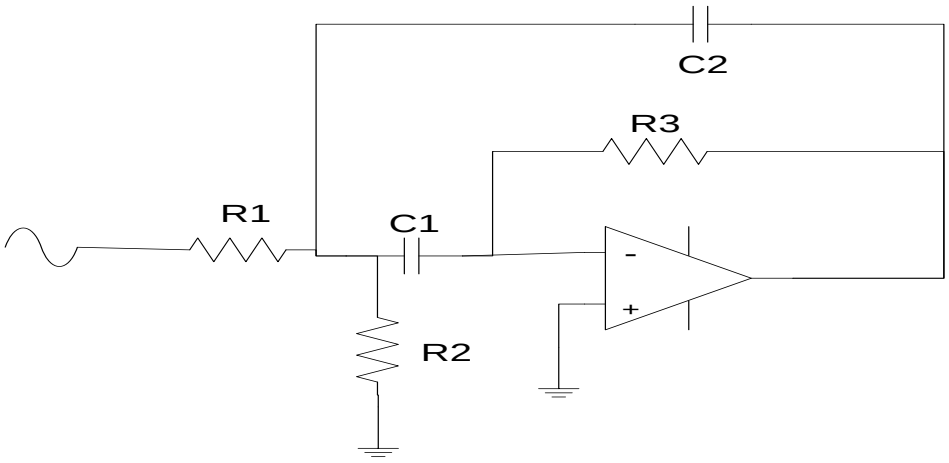

Components

R1 = 16.9kΩ

R2 = 43.3 Ω

R3 = 33.86kΩ

C1 = C2 = 0.47µF

TRITA-STH Report 2013: 105

www.kth.se